IET Microwaves, Antennas & Propagation

Research Article

IET Journals
The Institution of Engineering and Technology

Circularly polarised periodic leaky-wave antenna with filtering capability

ISSN 1751-8725
Received on 19th March 2018
Revised 6th April 2018
Accepted on 23rd April 2018
E-First on 15th May 2018
doi: 10.1049/iet-map.2018.0168
www.ietdl.org

Mohammad Hassan Rahmani[1] ✉, *Dominic Deslandes*[1]

[1]*Department of Electrical Engineering, Ecole de Technologie Superieure, Montreal, Canada*

✉ *E-mail: mohammadhassan.rahmani.1@ens.etsmtl.ca*

Abstract: A planar periodic leaky-wave antenna with filtering capability, circular polarisation, and wideband performance is presented. Seamless beam scanning from backward to forward is provided by self-matching the unit cell of the antenna over a large frequency band from 22 to 28 GHz. A wide scanning range of 84° is achieved by using a relatively low-permittivity dielectric material. Filtering capability is embedded in the antenna structure which contributes to the minimisation of the overall circuit size which is aimed in recent millimetre-wave antenna in package systems. The proposed antenna has a circular polarisation with an axial ratio of <2 dB at broadside which makes it a good candidate for peer-to-peer and peer-to-multipeer communication systems.

1 Introduction

Printed leaky-wave antennas have been able to regain researchers attention during the past few years [1–5]. They are compact, low profile, and their radiation beam can be steered by only changing the frequency of the input signal. The frequency dependency of the phase constant (i.e. β) leads to a sweep of the radiated beam and produces a frequency scanning antenna [6].

Periodic leaky-wave antennas (PLWA) are realised by cascading the unit cells (UC) in one direction. An infinite number of fast or slow space harmonics are then produced where the fast harmonics are the one that produce a radiation [6]. These antennas are able to scan the space from the backward to the forward quadrant leading to a full-space beam scanning. A PLWA is mainly characterised by its UC behaviour in terms of dispersion characteristics [6].

Several parameters, however, may limit the applicability of these antennas in mm-Wave (millimetre-wave) applications. Limited impedance bandwidth and scanning range, high scanning sensitivity with frequency, and lack of circular polarisation are the main shortcomings of the currently designed PLWA structure.

One of the most important problems that has been addressed thoroughly in recent years is the presence of an open stop band (OSB) at broadside frequency that degrades the gain of the radiated beam at this frequency. The suppression of this OSB has been rigourously addressed in many research works such as [1, 3, 7–10]. It has been demonstrated in [11] that the OSB can be mitigated by matching the input impedance of the UC with the characteristic impedance of the transmission line. As a result, a real input impedance is obtained which in turn leads to a constant and almost real Bloch impedance. However, finding a wideband and adjustable self-matching structure is an important challenge that has not been addressed previously.

Antenna circular polarisation is another crucial necessity of the antenna systems for mm-Wave peer-to-peer and peer-to-multipeer communication. In order to have a circular polarisation, an axial asymmetry needs to be present in the UC structure [2] to produce a phase quadrature relation between the series and shunt radiation components of the UC. By optimising the level of asymmetry and reaching a Q balance state, it is possible to minimise the axial ratio (AR) and achieve an almost circular polarisation [2]. However, the antennas presented in [2] are not discussed from the impedance bandwidth and scanning range point of view which can be limited by the narrowband performance of the single UC [12].

In [11], a circularly polarised PLWA is presented that has a wide steering angle of 95° (including the broadside) with low-frequency scanning sensitivity, wide impedance bandwidth of 47%, and an optimised side lobe level (SLL) of 13 dB at broadside. However, since there is no control over the impedance bandwidth of the UC, using this antenna in a communication system requires independent design of passive band-pass filters, thus increasing the overall size of the communication system. In mm-Wave communications, where antennas are to be integrated in multi-layer packages, the compactness of the passive components becomes crucial. Therefore, adding filtering function to the LWA by increasing its filtering order and controlling its pass-band region can be used to relax the filter specifications or even remove the first band-pass filter.

In this paper, we present a new circularly polarised printed PLWA based on the antenna presented in [11]. The single UC demonstrates a band-pass filter behaviour with three resonance frequencies. The centre frequency and the bandwidth of this filter can be adjusted using the structure parameters such as the length and the width of the UC. When the adjusted UC is cascaded to realise a PLWA, we are at the same time increasing the order of the band-pass filter and improving its performance [13]. Therefore, the performance of the antenna presented in [11] is improved by adding an open stub to the UC structure and increasing its filtering order.

This paper is organised as follows. In the second section, the design procedure of the UC is detailed where OSB suppression and band-pass filtering capability are described. A parametric study is performed on the UC to shed light on its important physical parameters for tuning the pass-band of the filter. Finally, we show that there is a good agreement between measured and simulated results with a wide scanning range and −10 dB impedance bandwidth.

2 UC analysis and parametric study

As it can be observed in Fig. 1*a*, the proposed antenna is realised by periodically repeating the UC structure along the direction of propagation. The UC itself is composed of a stepped impedance transmission line loaded with two shorting vias and an open stub with a slot.

Compared with the structure presented in [11], this UC has an open stub that adds a resonance frequency and increases the filtering order as depicted in Fig. 1*b*. The pass-band selectivity of the antenna is therefore increased with an elliptical transfer

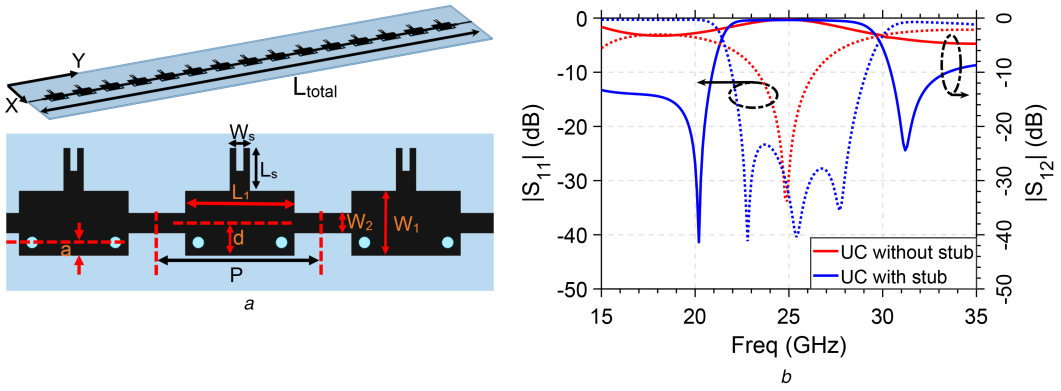

Fig. 1 *Presentation of the planar PLWA*
(a) Schematic view, ***(b)*** S_{11} and S_{12} of the UC with and without the open stub

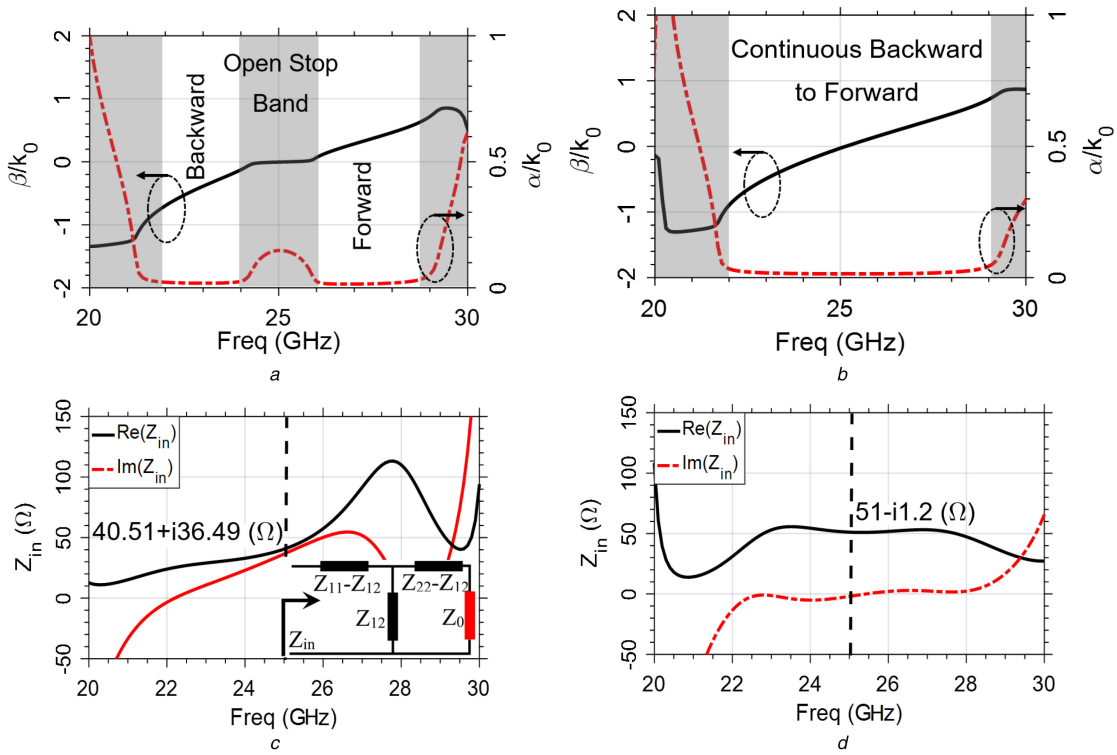

Fig. 2 *Dispersion characteristics and input impedance of the UC*
(a) Non-optimised UC, ***(b)*** Optimised UC, ***(c)*** Non-optimised UC input impedance, ***(d)*** Optimised UC input impedance

function response which causes sharper out-of-band rejection region. This interesting feature of the UC is the main advantage of this antenna compared with the antenna presented in [11]. The dimensions of this stub affect the frequency response of the UC and can be used to tune the filter.

The UC needs to be analysed both in terms of its input impedance and dispersion parameters. On the one hand, when the UC is matched with the transmission line over the desired bandwidth, the final PLWA will consequently have a good matching performance. On the other hand, its dispersion characteristic needs to be checked for the presence of the OSB.

2.1 OSB suppression

The dispersion curve of a periodic antenna can be derived using the Bloch wave analysis as described in [11]. The scattering parameters of a single UC are extracted using full-wave simulation with Ansys HFSS [14]. The complex propagation constant of an infinitely long periodic antenna is then extracted directly from the *S*-parameters. In order to account for the mutual coupling between the UCs, five cells have been simulated together to obtain the scattering matrix.

As it can be observed in Fig. 2*a*, the non-optimised UC has a stop band where the attenuation constant peaks at the centre frequency and the phase constant remains around zero. This stop band is caused by two oppositely directed space harmonics having the same amplitude and results in the increase in the VSWR and consequently, the degradation of the radiated beam at this frequency [6].

To suppress the OSB and obtain a seamless scanning through the broadside, it is required to match the input impedance of the UC with the characteristic impedance of the transmission line ($Z_0 = 50\,\Omega$) [3]. The equivalent network of Fig. 2*c* is obtained using full-wave simulation and used to extract Z_{in} of a single UC when it is terminated by Z_0:

$$Z_{in} = [(Z_0 + Z_{22} - Z_{12}) \parallel Z_{12}] + Z_{11} - Z_{12} \quad (1)$$

The resulted input impedance is presented in Fig. 2*c*. The unmatched UC has a Z_{in} with a large and variant imaginary part over the desired frequency range with a value of $40.51 + i36.49\,\Omega$ at the centre frequency. Therefore, a high imaginary part value of the Bloch impedance is produced at this frequency which in turns leads to a stop band and degrades the radiation performance of the resulted antenna [9].

The input impedance of the UC is mostly influenced by W_1, W_2, and d. By varying these dimension parameters, the UC can be

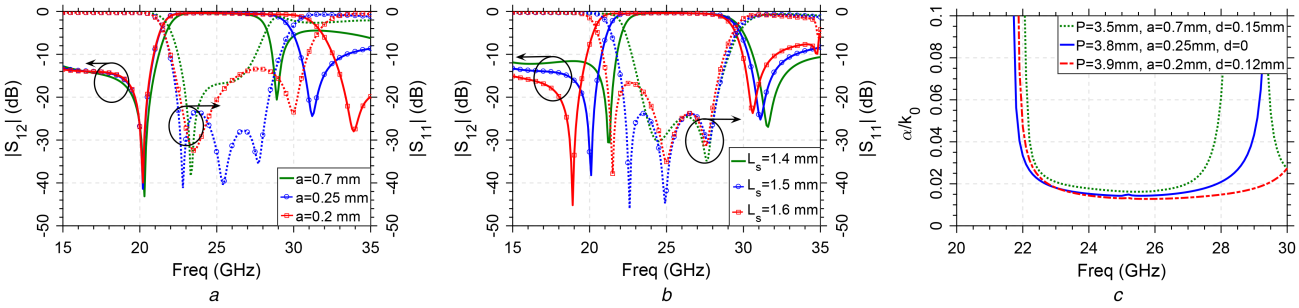

Fig. 3 *Effect of different physical dimension parameters on the behaviour of the UC*

(a) Distance of the vias from the border a (while $L_s = 1.5$ mm), ***(b)*** L_s length of the open stub (while $a = 0.25$ mm), ***(c)*** Position of the high impedance line relative to axial symmetry axis d (while $L_s = 1.5$ mm)

Table 1 Dimensions of the fabricated UC

Parameter name	P	L_1	a	d	L_s	W_s	W_2	W_1
dimensions, mm	5.8	3.8	0.25	0	1.5	0.7	0.7	2.3

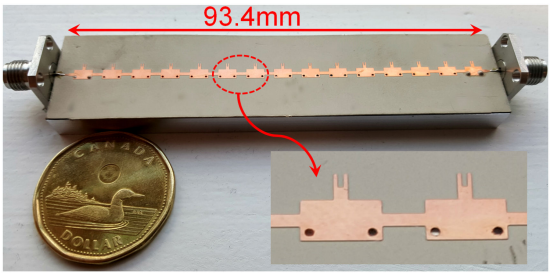

Fig. 4 *Fabricated antenna mounted on an aluminium base structure*

matched to have an almost real impedance over the frequency band which can be interpreted as inserting impedance transformers as demonstrated in [9]. The dispersion characteristics and input impedance of the optimised UC are shown in Figs. 2*b* and *d*. In this new structure, Z_{in} has an imaginary part close to zero with a real impedance of ∼50 Ω. Consequently, the OSB is eliminated resulting in a seamless radiation beam scanning over the frequency range of interest.

2.2 Parametric study

The UC can also be considered as a band-pass filter. A parametric study has been performed on one UC to understand its behaviour. The centre frequency of this filter can be adjusted by changing P (the period of the PLWA). Lower resonance frequency is achieved by increasing the length of the UC which in turns increases the length of the radiating edges.

The bandwidth of the filter is adjusted using a and L_s. The former varies the width of the high impedance line without varying the position of the shorting vias, while the latter is the length of the open stub. In fact, the open stub has two functions: (i) it increases the filtering order of the UC by adding a resonance frequency to the structure, and (ii) it serves as an adjusting parameter for controlling the bandwidth of the pass-band filter.

The distance of the feeding line centre from the edge of the UC, d, is used to adjust the matching of the UC and remove the OSB. The effect of each parameter on the performance of the UC is shown in Figs. 3*a*–*c*.

In order to suppress the OSB and simultaneously have a good input matching, all these parameters need to be optimised together. Using the above parametric study, a process flow is suggested for the design of an optimum UC that has a desired bandwidth and mitigated OSB. First, the distance a and L_s are adjusted to obtain the desired bandwidth. Higher values of a result in a smaller pass-band, while lower values of a lead to larger bandwidth. L_s modifies the position of the lower frequency resonance by changing the electrical length of the open stub. Lower values push the resonance to higher frequencies leading to a narrower bandwidth and vice versa. By varying a and L_s, the centre frequency of the UC is modified since its total area has changed causing a different length of the radiating edges. In order to compensate, the length P is adjusted to achieve the desired centre resonance frequency. Finally, when the desired bandwidth and centre frequency are obtained, the position of the feeding line is adjusted to match the input impedance of the UC to Z_0 and suppress the OSB. Other parameters such as W_s, W_2, and the dimensions of the slot affect the matching of the UC and can be used to fine tune the OSB suppression.

By using the above process, a UC has been designed that has a centre frequency of 25 GHz, and a bandwidth of ∼6 GHz from 22 to 28 GHz. The dimensions of the final optimised UC are presented in Table 1. By cascading 15 UCs, along the direction of propagation, a PLWA is achieved that can at the same time act as a band-pass filter and radiate only in the desired bandwidth and reject the undesired frequencies.

3 Antenna fabrication and measurement

The final PLWA is realised by cascading 15 optimised UCs. Two high-frequency 2.92 mm connectors are used to excite the antenna at one end, while the other end is grounded with a matched load. Each UC is optimised for the desired band-pass filter response without an OSB. Therefore, the final antenna will also be matched and OSB-free, while presenting a high-order pass-band behaviour with sharper rejection region than the structure presented in [11].

An *RO*3006 substrate with $\epsilon_r = 6.15$ and a height of 0.25 mm has been used to fabricate the antenna. Fig. 4 shows the fabricated antenna on an aluminium base which is used to increase the rigidity of the structure. A mm-Wave test fixture has been used to measure the S parameters of the antenna to be compared with full-wave simulation results in Fig. 5. It can be observed that there is a very good agreement between the measured and simulated S-parameters of the antenna. However, higher dielectric loss than the nominal value at mm-Wave frequencies, connector losses (∼0.1 dB), and defective shorting vias were identified as the possible error sources for an accurate full-wave simulation.

The radiation patterns are measured in an anechoic chamber and depicted in Fig. 6 from 22 to 28 GHz. A good agreement is preserved between the simulation and measurement results in terms of scanning angle and continuous scanning which is realised by eliminating the OSB at broadside frequency. The steering angle is from −44° at 22 GHz to 40° at 28 GHz providing a wide scanning angle of 84° from backward to forward direction. The maximum gain variation is 2.8 dB throughout the steering range. However, there is ∼2 dB difference in lower frequencies, and ∼4 dB in higher frequencies between the measured radiation gain and the simulated results. This is mainly due to losses caused by connectors and other measurement inaccuracies. An SLL of about −7 dB can be observed in Fig. 6 which is mainly caused by the

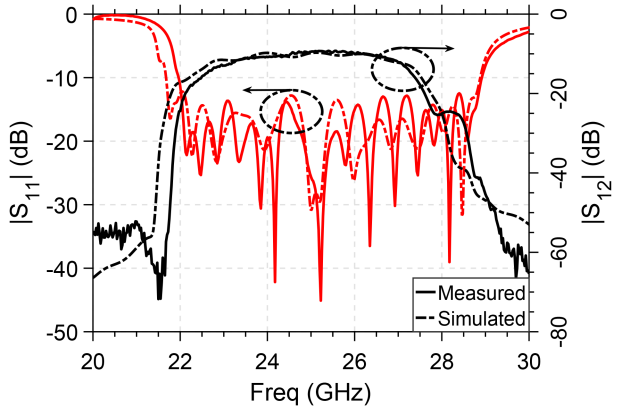

Fig. 5 *Amplitude of S_{11} and S_{12} of the final simulated and fabricated antenna*

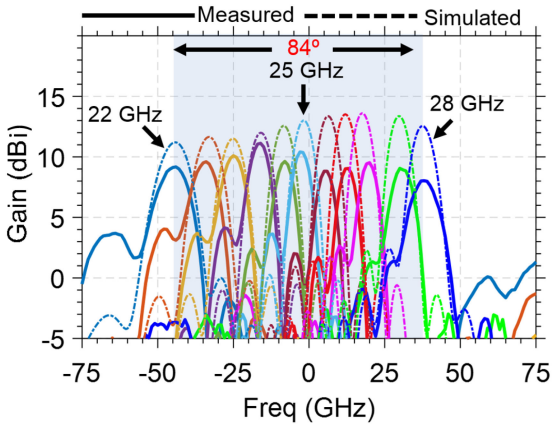

Fig. 6 *Measured and simulated radiation pattern of the antenna for a frequency variation from 22 to 28 GHz*

limited number of UCs that are used in the antenna structure. This problem can be solved by tapering the amplitude of the aperture distribution as discussed in [11]. The shunt and series radiation components of the UC are in phase quadrature which in turns lead to a circular polarisation of the total radiation pattern. As shown in Fig. 7, the AR of the final antenna is ~1 dB for the scanning range except the scanning borders where one radiation component is attenuated by approaching the scanning bounds. A good agreement can be observed between simulated and measured results in this figure. This value of AR is low enough for various applications that need circular polarisation. In order to compare the AR performance of this structure with the no-stub antenna [11], the simulated AR of this antenna is also shown in Fig. 7. As it can be observed, for both structures the AR level increases for out-of-band regions. For the UC without the stubs, the AR enters the <3 dB region at ~22.5 GHz, while for the UC with the stubs, it enters this region at 23.2 GHz. Unfortunately, compared with the impedance bandwidth, both structures show a narrower 3 dB AR bandwidth. However, for the proposed structure, the AR bandwidth is closer to the impedance bandwidth which means that adding the stubs to the UC does not interfere with the AR bandwidth performance.

The co-polarised (RHCP) and cross-polarised (LHCP) radiation patterns are depicted in Fig. 8*a*. The maximum cross-polarisation rejection level is about −20 dB at broadside and it decays according to the AR value for off-broadside frequencies. The simulated surface current density is also demonstrated in Fig. 8*b* where the counter-clockwise rotation of the main current vector shows the RHCP polarisation direction of the antenna.

The average radiation efficiency of the simulated antenna is ~52% over the desired frequency range as shown in Fig. 9. The low value of $|S_{21}|$ (i.e. about −10 dB) also confirms this efficiency value. In order to have a more efficient antenna, the number of UCs can be increased so that a greater portion of the power is radiated before the wave reaches the end of the PLWA at port 2. Another way of increasing the radiation efficiency is to increase the leakage

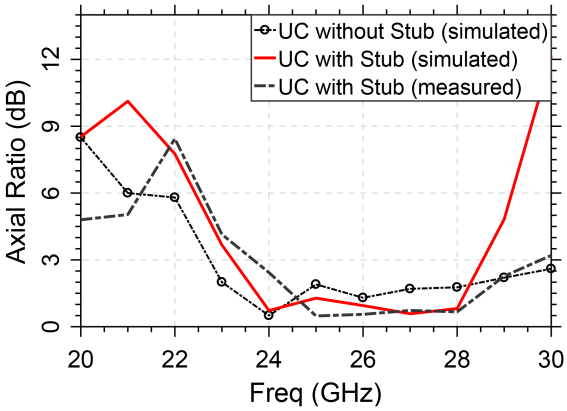

Fig. 7 *AR of the final antenna for different frequencies*

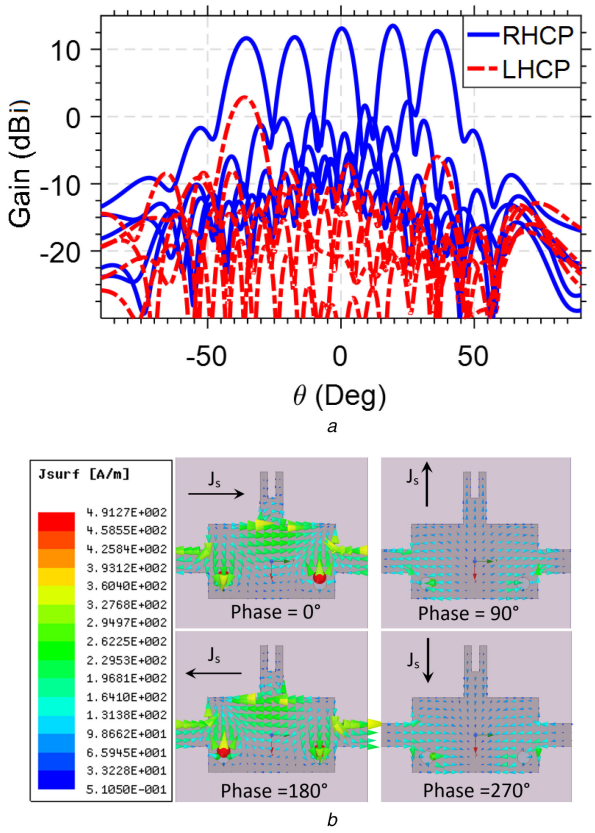

Fig. 8 *Co-polar (RHCP) and cross-polar (LHCP) radiation patterns of the antenna*

(a) Simulated radiation patterns, ***(b)*** Simulated surface currents with the direction of the dominant current showing the counter-clockwise (RHCP) rotation of the currents

constant. In this structure, this can be realised by placing the shorting vias closer to the centre axis of the UC as demonstrated in [11]. Therefore, based on the desired application, the antenna can be optimised to provide a higher radiation efficiency. The amount of power loss in the measured and simulated antenna, presented in Fig. 9, confirms the broadband behaviour of the matched antenna with a high level of accepted power. The high value of this ratio indicates that a small fraction of the power is reaching port 2.

Table 2 summarises the performance characteristics of the proposed antenna and compares it with the recently proposed PLWAs with circular polarisation. The main contribution of this work, which is a sharp rejection for out-of-band frequencies, is not discussed in these works. Moreover, usually the pass-band boundaries of the PLWAs presented in [5, 15, 16] are not easily adjustable for various applications. The scanning range of our proposed prototype is higher than [15, 16] but less than [5], although gain variations of this publication are higher over the bandwidth. In a more recent work [17], a low-profile microstrip leaky-wave antenna is proposed with a filter-like frequency

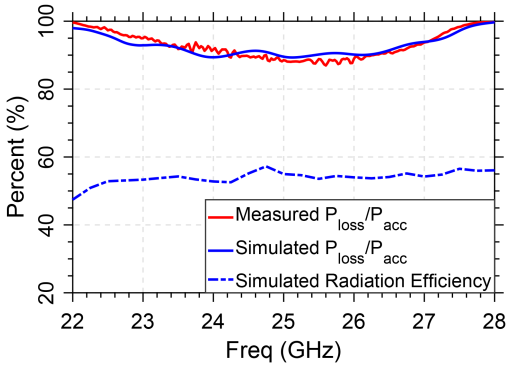

Fig. 9 *Ratio of $P_{loss} = 1 - |S_{11}|^2$ over $P_{acc} = 1 - |S_{11}|^2 - |S_{21}|^2$ for the simulated and measured antenna (solid lines), and the simulated radiation efficiency (dot-dashed line)*

Table 2 Comparison with other circularly polarised PLWA configurations

Structure	Antenna type	scanning range, deg	Bandwidth, GHz	Polarisation	Adjustable filtering capability
[5]	half-mode SIW	−70 to +70	7.4–13.5	circular	no
[15]	CRLH SIW	−40 to +25	10–14	circular	no
[16]	CRLH SIW	−29 to +24	4.2–4.85	circular	no
[11]	printed microstrip	−50 to +45	20–29	circular	no
this work	printed microstrip	−44 to +40	22–28	circular	yes

response, comparable scanning range, and impedance bandwidth to our work. However, our current work has the advantage of being circularly polarised with a good axial radiation bandwidth which makes it a better candidate for mm-Wave communication systems. Moreover, the controlling parameters of the bandwidth are not presented in [17].

4 Conclusion

A new PLWA structure with filtering capability, wideband performance, and circular polarisation has been proposed in this letter. Continuous gain steering from backward to forward quadrant is realised by matching the Z_{in} of the single UC to 50 Ω leading to a purely real Bloch impedance.

The UC is self-matched using the step discontinuities and shorting vias over a large frequency band, making it needless of a separate matching structure to suppress the OSB. A wide scanning range with a low scanning sensitivity is achieved by using a relatively low ε_r compared to other PLWA structures in the literature. Moreover, due to the asymmetry of the UC, the antenna has a circular polarisation where its AR can be optimised by varying the asymmetry parameters.

Adjustable filtering capability is another interesting feature of this antenna which is made possible by using an open stub in the UC. The single UC acts as a band-pass filter with three resonance frequencies. The cascade of several UCs increases the order of the filter and improves its out-of-band rejection behaviour. The bandwidth of the filter is controlled by varying the dimensions of the open stub as well as the width of the patch to tailor the antenna for various mm-Wave applications.

The final PLWA has a circular polarisation with a relatively low AR over the bandwidth, adjustable filtering capability, wide scanning range with low scanning sensitivity, and wide impedance bandwidth. These interesting features, together with a simple design and fabrication process, make this antenna a good candidate for various mm-Wave scanning applications.

5 References

[1] Henry, R., Okoniewski, M.: 'A broadside scanning substrate integrated waveguide periodic phase-reversal leaky-wave antenna', *IEEE Antennas Wirel. Propag. Lett.*, 2015, **15**, pp. 602–605

[2] Otto, S., Chen, Z., Al-Bassam, A., *et al.*: 'Circular polarization of periodic leaky-wave antennas with axial asymmetry: theoretical proof and experimental demonstration', *IEEE Trans. Antennas Propag.*, 2014, **62**, (4), pp. 1817–1829

[3] Rahmani, M.H., Deslandes, D.: 'A novel periodic microstrip leaky-wave antenna with backward to forward scanning'. 2015 IEEE-APS Topical Conf. on Antennas and Propagation in Wireless Communications (APWC), Torino, Italy, 2015, pp. 650–653

[4] Rance, O., Lemaître Auger, P., Siragusa, R., *et al.*: 'Generalized array factor approach to the assessment of discrete tapered nonuniform leaky-wave antenna', *IEEE Trans. Antennas Propag.*, 2015, **63**, (9), pp. 3868–3877

[5] Saghati, A.P., Mirsalehi, M.M., Neshati, M.H.: 'A HMSIW circularly polarized leaky-wave antenna with backward, broadside, and forward radiation', *IEEE Antennas Wirel. Propag. Lett.*, 2014, **13**, pp. 451–454

[6] Jackson, D.R., Oliner, A.A.: 'Leaky-wave antennas', in Balanis, Constantine A. (Eds.): '*Modern antenna handbook*', vol. **1** (Wiley-Blackwell, USA, 2008), pp. 325–368

[7] Ning, Y., Caloz, C., Ke, W.: 'Full-space scanning periodic phase-reversal leakywave antenna', *IEEE Trans. Microw. Theory Tech.*, 2010, **58**, (10), pp. 2619–2632

[8] Otto, S., Al-Bassam, A., Rennings, A., *et al.*: 'Transversal asymmetry in periodic leaky-wave antennas for Bloch impedance and radiation efficiency equalization through broadside', *IEEE Trans. Antennas Propag.*, 2014, **62**, (10), pp. 5037–5054

[9] Paulotto, S., Baccarelli, P., Frezza, F., *et al.*: 'A novel technique for open-stopband suppression in 1-D periodic printed leaky-wave antennas', *IEEE Trans. Antennas Propag.*, 2009, **57**, (7), pp. 1894–1906

[10] Williams, J.T., Baccarelli, P., Paulotto, S., *et al.*: '1-D combline leaky-wave antenna with the open-stopband suppressed: design considerations and comparisons with measurements', *IEEE Trans. Antennas Propag.*, 2013, **61**, (9), pp. 4484–4492

[11] Rahmani, M.H., Deslandes, D.: 'Backward to forward scanning periodic leakywave antenna with wide scanning range', *IEEE Trans. Antennas Propag.*, 2017, **65**, (7), pp. 3326–3335

[12] James, J.R., Hall, P.S., Wood, C.: '*Microstrip antenna: theory and design*' (IET, UK, 1981)

[13] Pozar, D.M.: '*Microwave engineering*' (John Wiley & Sons, USA, 2009)

[14] Ansoft, H.: '*Users guide high frequency structure simulator*' (Ansoft Co., USA, 2003)

[15] Lyu, Y.L., Meng, F.Y., Yang, G.H., *et al.*: 'Periodic SIW leaky-wave antenna with large circularly polarized beam scanning range', *IEEE Antennas Wirel. Propag. Lett.*, 2017, **16**, pp. 2493–2496

[16] Lee, H., Choi, J.H., Wu, C.T.M., *et al.*: 'A compact single radiator CRLH-inspired circularly polarized leaky-wave antenna based on substrate-integrated waveguide', *IEEE Trans. Antennas Propag.*, 2015, **63**, (10), pp. 4566–4572

[17] Lyu, Y.-L., Meng, F.-Y., Yang, G., *et al.*: 'Leaky-wave antenna with alternately loaded complementary radiation elements', *IEEE Antennas Wirel. Propag. Lett.*, 2018, **17**, pp. 679–683